

NUMERICAL SIMULATION OF PHOTOCURRENT IN A SOLAR CELL BASED AMORPHOUS SILICON

E. Ihalane^{*1}, M. Meddah¹, A. Elfanaoui¹, L. Boulkaddat¹, E. El hamri¹, X. Portier², A. Ihlal¹ and K. Bouabid¹

¹ LABORATOIRE MATÉRIAUX ET ENERGIES RENOUVELABLES (LMER), UNIVERSITÉ IBN ZOHR DÉP. PHYSIQUE, FACULTÉ DES SCIENCES B.P.8106, HAY DAKHLA, 80000 AGADÏR, MAROC.

² CiMAP ENSICAEN, 6 Bd du Maréchal Juin 14050 Caen cedex, France.

*corresponding author: hassanihalane@gmail.com

Keywords: Amorphous silicon; a-Si:H; Photovoltaic parameters ; AMPS-1D; Single junction.

Abstract: We propose in this work, a method of simulation based on the resolution of the equations of continuities for homostructures of silicon-based solar, and used a method of calculation the photocurrent delivered by the silicon solar cell applying the equations of continuities and the currents by analogy to the phenomena of loads transport according to the model of an homojunction n-a-Si:H/p-a-Si:H. We used Matlab software to simulate and optimize the layers thicknesses to achieve the maximum photocurrent generated under AM1.5 solar spectrum. The optimization of donor layer thickness shows clearly that the best results are obtained with the finest structures. We worked out a numerical model based on the resolution of the equations of continuities who gave the results in good agreement with literature and which allowed, moreover a better control of the performances of the cells based on silicon, for their improvement.

I-Introduction

Hydrogenated amorphous silicon (a-Si:H) has drawn considerable attention worldwide because of its potential use in fabricating large-area, low-cost devices such as thin film solar cells, thin film transistors, radiation detectors, liquid crystal displays, ect. The initial photo J-V characteristics for the fabricated p-i-n type a-Si:H solar cells on both Asahi U-type glass substrates and PET/ITO plastic substrates. At the low temperature of 125°C, flexible a-Si:H solar on PET substrate with an efficiency of 4.60% ($V_{oc}=0.98V$, $FF=0.69$, $J_{sc} = 6.82mA/cm^2$) [1].

Analysis of Microelectronic and Photonic Structures (AMPS-1D) is a very general program for analyzing and designing transport in microelectronic and photonic structures [2]. It has proved to be a very powerful tool in understanding device operation and physics for single crystal, poly-crystalline and amorphous structures [3].

The one-dimensional device simulation program AMPS-1D solves the Poisson equation and the electron and hole continuity equations by using finite differences and the Newton-Raphson[4]

II-Simulation model

In a one-dimensional semiconductor device, the device physics operation can be described by solving Poisson's equation, and the electron and hole continuity equations at each position throughout the device[5]. AMPS-1D simulator

has been employed to model and analyze the solar cell as shown in fig.1.

In this work we used the AMPS-1D for simulation of solar cell performance. Variation of efficiency, open circuit voltage (V_{oc}), short-circuit current (J_{sc}) and fill factor (FF) with the variation of thickness and doping concentrations of different layers. For a-Si:H we obtained data from the AMPS-1D parameter compendium and from literature, the values of different material parameters used in AMPS-1D are show in tables 1 and 2.

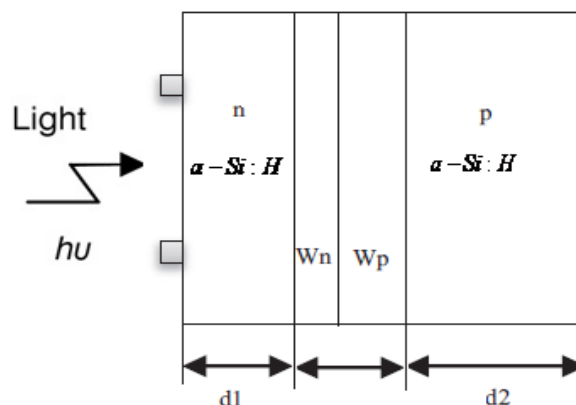


Fig 1: Schema diagram of the homo-junction amorphous silicon structure.

Table 1: Parameter set for simulation of homo-junction solar cells with AMPS-1D [4-7].

Parameters	n-a-Si:H	p-a-Si:H	i-a-Si:H
Layer thickness L(nm)	10	280	10
Mobility band gap E_g (eV)	1.8	1.8	1.8
Electron affinity χ (eV)	4	4	4
Donor doping density N_D (cm^{-3})	1×10^{19}	0	0
Acceptor doping density N_A (cm^{-3})	0	1.5×10^{19}	0
Effective conduction band density (cm^{-3})	2.5×10^{20}	2.5×10^{20}	2.5×10^{20}
Effective valence band density (cm^{-3})	2.5×10^{20}	2.5×10^{20}	2.5×10^{20}
Capture cross-section for donor states, electron (cm^2)	1×10^{-15}	1×10^{-15}	1×10^{-15}
Capture cross-section for donor states, holes (cm^2)	1×10^{-17}	1×10^{-17}	1×10^{-17}
Electron mobility μ_e (cm^2 / Vs)	20	20	20
Hole mobility μ_h (cm^2 / Vs)	2	2	2
Characteristic energy (eV) for donors	0.05	0.05	0.05
Characteristic energy (eV) for acceptors	0.03	0.03	0.03

Table 2: Contact parameters as used in the simulation.

Parameters	Front contact	Back contact
Barrier height ϕ_b (eV)	1.9	0.03
Electron recombination velocity S_n (cm / s)	1×10^7	1×10^7
Electron recombination velocity S_p (cm / s)	1×10^7	1×10^7
Reflection coefficient	0.10	0.90

III-Photocurrent densities

The photocurrent density is calculated from the concentration of the minority carrier as follows[6]:

- For the holes in n-type region

$$J_p = qD_p \frac{\partial p(x)}{\partial x} \quad (1)$$

- For the electrons in the p-type region

$$J_n = -qD_n \frac{\partial n(x)}{\partial x} \quad (2)$$

Where $p(x)$ is the holes concentration in n-type layer, and $n(x)$ is the electrons concentration in p-type layer. D_p and D_n are the holes and electrons diffusion coefficient, respectively.

The concentration of the excess minority carrier (holes) is given by :

$$p(x) = \left[\alpha(\lambda) F(\lambda) (1 - R(\lambda)) \tau_p / (\alpha(\lambda)^2 L_p^2 - 1) \right] \times \left[\frac{\left(\frac{S_p L_p}{D_p} + \alpha(\lambda) L_p \right) \sinh\left(\frac{d_1 - x}{L_p}\right) + \exp(-\alpha(\lambda) d_1) \left[\frac{S_p L_p}{D_p} \sinh\left(\frac{x}{L_p}\right) + \cosh\left(\frac{x}{L_p}\right) \right]}{\frac{S_p L_p}{D_p} \sinh\left(\frac{d_1}{L_p}\right) + \cosh\left(\frac{d_1}{L_p}\right)} \right] \exp(-\alpha(\lambda) x) \quad (3)$$

Where $R(\lambda)$ is reflection coefficient, $\alpha(\lambda)$ is the absorption coefficient, $F(\lambda)$ is photon flux, S_p, S_n are the holes and electron velocity respectively, τ_p, τ_n are the holes and electron lifetime respectively, and L_p, L_n are the holes and electron diffusion length respectively.

The photocurrent density produced at $x = d_1$ is given by:

$$J_p(\lambda) = \left[qF(\lambda)(1-R(\lambda))\alpha(\lambda)L_p / (\alpha(\lambda)^2 L_p^2 - 1) \right] \times \left[\frac{\left(\frac{S_p L_p}{D_p} + \alpha(\lambda)L_p \right) - \exp(-\alpha(\lambda)d_1) \left[\frac{S_p L_p}{D} \cosh\left(\frac{d_1}{L_p}\right) + \sinh\left(\frac{d_1}{L_p}\right) \right]}{\frac{S_p L_p}{D_p} \sinh\left(\frac{d_1}{L_p}\right) + \cosh\left(\frac{d_1}{L_p}\right)} - \alpha(\lambda)L_p \exp(-\alpha(\lambda)d_1) \right] \quad (4)$$

The concentration of the excess minority carrier (electrons) is given by :

$$n(x) = \frac{\alpha(\lambda)F(\lambda)(1-R(\lambda))\tau_n}{\alpha^2 L_n^2 - 1} \exp[-\alpha(\lambda)(d_1 + w)] \times \left[\cosh\left(\frac{x - d_1 - w}{L_n}\right) - \exp[-\alpha(\lambda)(d_1 + w)] \right] - \frac{\left(\frac{S_n L_n}{D_n} \right) \left[\cosh\left(\frac{d_2}{L_n}\right) - \exp(-\alpha(\lambda)d_2) \right] + \sinh\left(\frac{d_2}{L_n}\right) + \alpha(\lambda)L_n \exp(-\alpha(\lambda)d_2)}{\frac{S_n L_n}{D_n} \sinh\left(\frac{d_2}{L_n}\right) + \cosh\left(\frac{d_2}{L_n}\right)} \times \sinh\left(\frac{x - d_1 - w}{L_n}\right) \quad (5)$$

The photocurrent density from the base due to electrons collected at the edge of junction $x = d_1 + d_2 + w$ is given by:

$$J_n(\lambda) = \frac{qF(\lambda)(1-R(\lambda))\alpha(\lambda)L_n}{(\alpha(\lambda)^2 L_n^2 - 1)} \exp[-\alpha(\lambda)(d_1 + w)] \times \left[\alpha(\lambda)L_n - \frac{\left(\frac{S_n L_n}{D_n} \right) \left[\cosh\left(\frac{d_2}{L_n}\right) - \exp(-\alpha(\lambda)d_2) \right] + \sinh\left(\frac{d_2}{L_n}\right) + \alpha(\lambda)L_n \exp(-\alpha(\lambda)d_2)}{\frac{S_n L_n}{D_n} \sinh\left(\frac{d_2}{L_n}\right) + \cosh\left(\frac{d_2}{L_n}\right)} \right] \quad (6)$$

The photocurrent density due to the space charge region

$$J_{scr}(\lambda) = qF(\lambda)(1-R(\lambda)) \exp(-\alpha(\lambda)d_1) [1 - \exp(-\alpha(\lambda)w)] \quad (7)$$

4-Simulation results and discussion

4-1-Simulation results of the photocurrent densities

The photocurrent densities in each abscissa of the cell were simulated versus the different layers abscissas under the solar spectrum Air Mass 1.5 (AM1.5). The equations (4), (6), (7) represents the photocurrent densities J_p , J_n and J_{scr} of the layers n-a-Si:H, p-a-Si:H and space charge regions. We computed the three photocurrent densities varying the layers thickness until we reach the maximum value of their sum J .

Fig.2 shows the first layer (n-a-Si:H) thickness optimization; it gives the total photocurrent density (the upper curve) generated by the cell solar versus the thickness d_1 . The maximum photocurrent density is obtained for a n-type layer equals 9.2 mA/cm^2 for $d_1 = 13 \text{ nm}$.

Fig. 3 represents the layer p-a-Si:H thickness optimization; the maximum photocurrent density for this layer equals 9.3 mA/cm^2 and optimal abscissa is $d_2 = 250 \text{ nm}$.

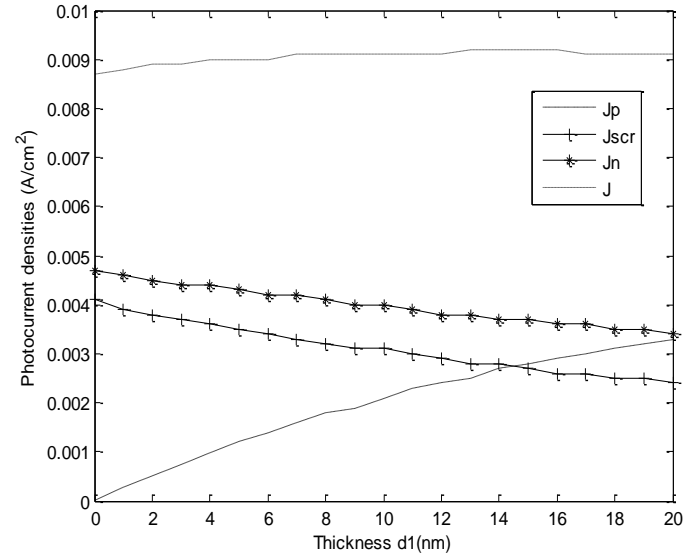


Fig 2 : Optimization of the layer n-a-Si :H thickness : the figure represents the photocurrents versus the thickness of the first layer d_1 , the photocurrent density J is the upper curve. The optimal abscissa is $d_{1,opt} = 13 \text{ nm}$.

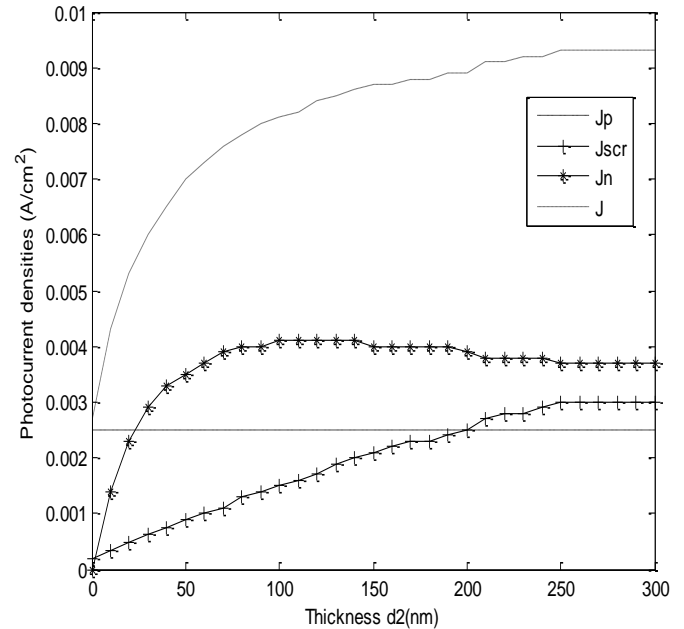


Fig 3 : Optimization of the layer p-a-Si :H thickness : the figure represents the photocurrents versus the thickness of the second layer d_2 , the photocurrent density J is the upper curve. The optimal abscissa is $d_{2,opt} = 250 \text{ nm}$.

4-2-Effect of thickness p-layer in performance

Fig.4 shows the variation of V_{oc} , J_{sc} , FF, and efficiency in single junction n-p solar cell with change of p-layer thickness in the range 10-110 nm. The maximum efficiency of 7.155% was found at thickness of 80nm. J_{sc} increased till 110 nm. FF and V_{oc} gradually decreased.

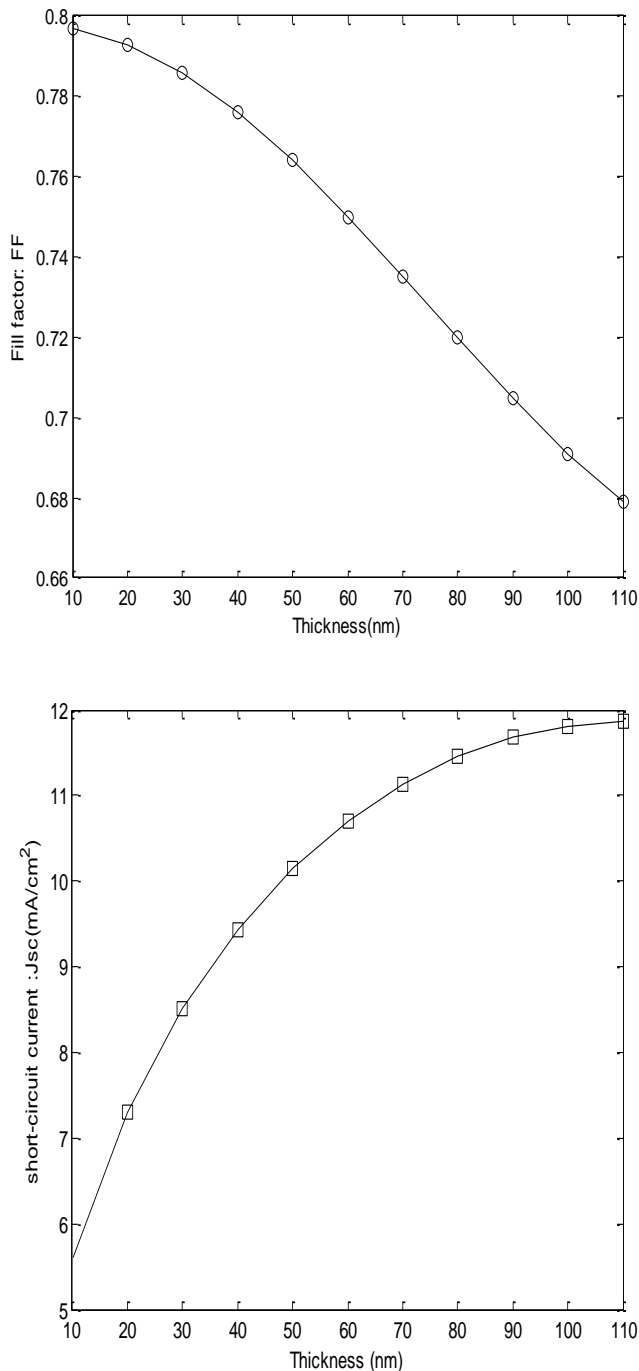


Fig.4.a Effect of thickness d_2 in fill factor (FF)

Fig.4.b Effect of thickness d_2 in short-circuit current in single junction cell n-a-Si:H/p-a-Si:H (J_{sc}) in single junction cell n-a-Si:H/p-a-Si:H

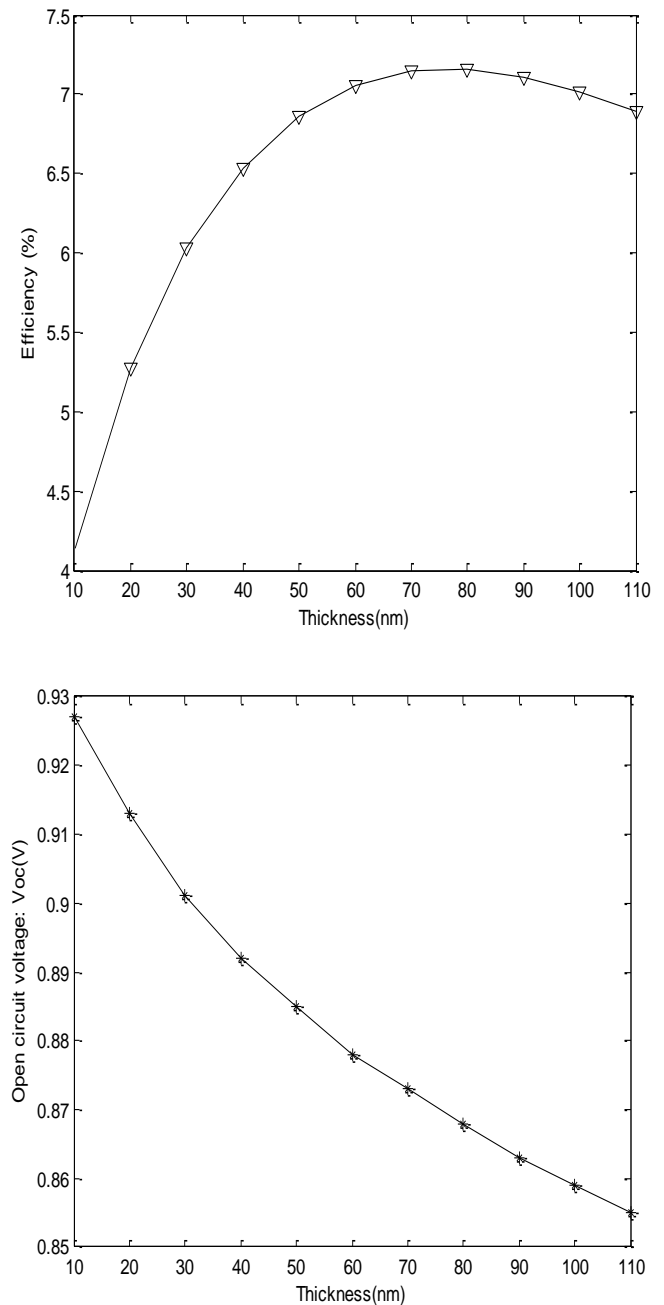


Fig.4.c Effect of thickness d_2 in efficiency in single junction cell n-a-Si:H/p-a-Si:H.

Fig.4.d Effect of thickness d_2 in open circuit voltage single in single junction cell n-a-Si:H/p-a-Si:H.

4-3- Effect of acceptor concentration in efficiency

The efficiency of the homo-junction n-i-p solar cell increased with the increase of the acceptor concentration. The efficiency reached its highest value of 10.192% at a acceptor concentration of $1.5 \times 10^{19} \text{ cm}^{-3}$ at shown in fig.5.

4-4- Effect of i-layer thickness in efficiency

Simulation curves of fig.6 show that the variation of acceptor concentration mainly affect on the efficiency. Higher efficiency has been simulated for cells with doping of $2 \times 10^{19} \text{ cm}^{-3}$ compared to the one simulated for cells with doping of $1 \times 10^{13} \text{ cm}^{-3}$ and of $1 \times 10^{21} \text{ cm}^{-3}$.

Conclusion

In this work, we have simulated a-Si:H homo-junction single using AMPS-1D. From the simulation, the efficiencies of the single junction n-a-Si:H/p-a-Si:H, n-a-Si:H/I-a-Si:H/p-a-Si:H are found to be 7.155%, 10.192%, respectively. These simulations allow to study the effect of the physical parameters on the photocurrent in order to choose suitable device parameters permitting an improvement of the solar cell performance. The optimization of donor layer thickness shows clearly that the best results are obtained with the finest structures.

References

- [1] Jian Ni, Jianjun Zhang* et al, Low teperature deposition of high open-circuit voltage ($>1.0 \text{ V}$) p-i-n type amorphous silicon solar cells, *Solar Energy Materials & Solar Cells* (2011) 1922-1926.
- [2] S.Fonash J. Arch, J. Hou, W. Howland, P. McElheny, A. Moquin, M. Rogosky, T. Tran, H. Zhu, F. Rubinelli, A Manual for AMPS-1D for Windows 95/NT a One-Dimensional Device Simulation Program for the Analysis of Microelectronic and Photonic Structures, The Pennsylvania State University.
- [3]Hong Zhu, Ali Kaan Kalkan, Jingya Hou and Stephen J Fonash, Applications of AMPS-1D for Cell Simulation, The Pennsylvania State University.
- [4]Norberto Hernandez-Como, Arturo Morales-Acevedo, Simulation of hetero-junction silicon solar cells with AMPS-1D, *Solar Energy Materials & Solar Cells* (2010) 62-67.
- [5] I.Bouchama, K. Djessas, F. Djahli, A.Bouloufa, Simulation approach for studying the performances of original superstrate CIGS thin films solar cells.
- [6]A. Bouhdada, R. Marrah, F. Vigué, J.-P. Faurie, Modeling of the spectral response of PIN photodetectors Impact of exposed zone thickness, surface recombination velocity and trap concentration, *Microelectronics Reliability* 44(2004) 223-228.
- [7] Abbas Belfar and Rachida Mostefaoui, Simulation of n1-P2 Microcrystalline Silicon Tunnel Junction with AMPS-1D in a-Si:H/ $\mu\text{c-Si:H}$ Tandem Solar Cells, *Journal of Applied Sciences* (2011) ISSN 1812-5654

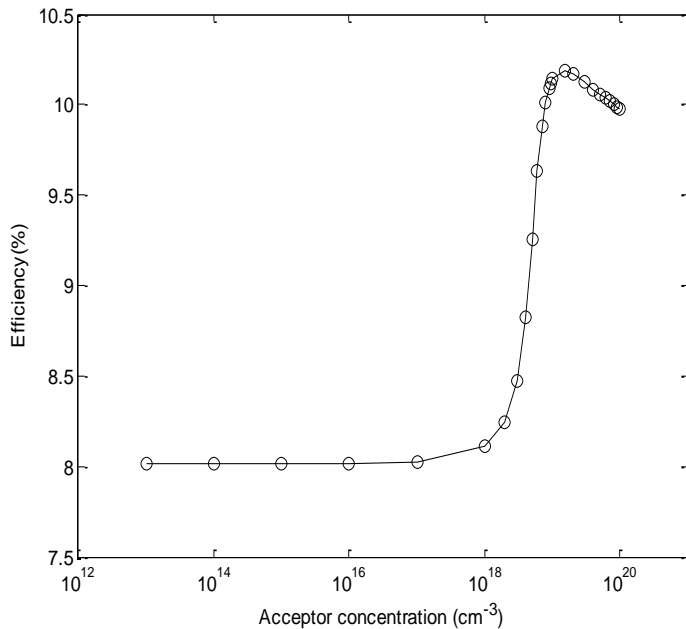


Fig 5: Effect of acceptor concentration (p-layer) on cell efficiency.

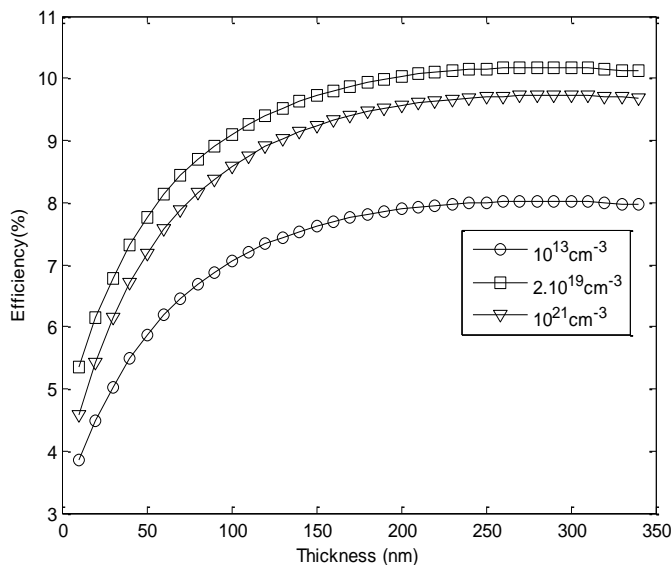


Fig 6: Effect of i-layer thickness in efficiency in cell n-a-Si:H/i-a-Si:H/p-a-Si:H